Inorganic Chemistry
Article

Inorg. Chem. **2009**, *48*, 6117–6123 **6117**
DOI: 10.1021/ic900470h

Diruthenium Tetracarbonate Trianion, $[Ru_2^{II/III}(O_2CO)_4]^{3-}$, Based Molecule-Based Magnets: Three-Dimensional Network Structure and Two-Dimensional Magnetic Ordering

Bretni S. Kennon,[†] Jae-Hyuk Her,[‡,§] Peter W. Stephens,[*,‡] and Joel S. Miller[*,†]

[†] *Department of Chemistry, 315 S. 1400 E. RM 2124, University of Utah, Salt Lake City, Utah 84112-0850, and*
[‡] *Department of Physics and Astronomy, Stony Brook University, Stony Brook, New York 11794*
[§] *Current address: Department of Materials Science and Engineering, University of Maryland, College Park, MD 20742-2115, U.S.A. and NIST Center for Neutron Research, National Institute of Standard and Technology, Gaithersburg, MD 20899-6102, U.S.A.*

Received March 9, 2009

$H_xK_{1-x}M^{II}[Ru_2(CO_3)_4](H_2O)_y(MeOH)_z$ (M = Mn, Fe, Co, Ni, Mg) were synthesized from the reaction of M^{II} and $K_3[Ru_2(CO_3)_4]$ in water and are isomorphous with an orthorhombic three-dimensional network structures based on μ_3-CO_3^{2-} linkages to Ru_2 moieties forming layers and also to *trans*-$M^{II}(OH_2)_4$ sites forming linked chains that connect the layers. They, as well as non-isomorphous M = Cu, magnetically order as canted ferrimagnets with $T_c = 4.4 \pm 1.0$ K. The presence of $S = 0$ M^{II} = Mg(II) has essentially no effect on T_c suggesting that the main magnetic pathway does not occur the through M^{II}-based chains, but only via $Ru_2 \cdots Ru_2$ linkages that reside in layers. This is a rare example of a magnet based upon a second row transition metal.

Introduction

The use of a D_{4h} paddlewheel-structured dimeric ruthenium species as a molecular building block to develop new molecule-based magnets has led to a new area of research.[1] Initial studies focused on the diruthenium tetracarboxylate cation, $[Ru_2(O_2CR)_4]^+$,[1-3] as (1) it has $S = 3/2$ ground state with the $\sigma^2\pi^4\delta^2\delta^{*1}\pi^{*2}$ valence electronic configuration, because of near degeneracy of the π^* and δ^* orbitals,[4] and an unusually large zero-field splitting, D,[4b,5,6] and (2) each Ru is pentacoordinate, and thus able to coordinate to an additional ligand, which is essential for building extended network structures. Various structural motifs can be obtained depending on the nature of the bridging carboxylate ligand. For example, acetate forms three-dimensional (3-D) interpenetrating structures,[1d,1e] while pivalate (O_2C^tBu) forms two-dimensional (2-D) layered motifs with $[Cr(CN)_6]^{3-}$.[1c] In addition to cationic Ru_2 carboxylates, anionic Ru_2-based species are known,[7-9] and their study may lead to additional structural motifs and possibly contribute to a better understanding of magnetic behavior. Recent work has shown $[Ru_2^{II/III}(CO_3)_4]^{3-}$ has great potential as a building block for

*To whom correspondence should be addressed. E-mail: jsmiller@chem.utah.edu.

(1) (a) Her, J.-H.; Kennon, B. S.; Shum, W. W.; Stephens, P. W.; Miller *Inorg. Chim. Acta* **2008**, *361*, 3462. (b) Kennon, B. S.; Her, J.-H.; Stephens, P. W.; Shum, W. W.; Miller, J. S. *Inorg. Chem.* **2007**, *46*, 9033. (c) Vos, T. E.; Miller, J. S *Angew. Chem., Int. Ed.* **2005**, *44*, 2416. (d) Vos, T. E.; Liao, Y.; Shum, W. W.; Her, J.-H.; Stephens, P. W.; Reiff, W. M.; Miller, J. S. *J. Am. Chem. Soc.* **2004**, *126*, 11630. (e) Liao, Y.; Shum, W. W.; Miller, J. S. *J. Am. Chem. Soc.* **2002**, *124*, 9336.
(2) (a) Aquino, M. A. S. *Coord. Chem. Rev.* **1998**, *170*, 141. (b) Buslaeva, T. M.; Redkina, S. N.; Rudnitskaya, O. V. *Russ. J. Coord. Chem.* **1999**, *25*, 3. (c) Aquino, M. A. S. *Coord. Chem. Rev.* **2004**, *248*, 1025.
(3) Yoshioka, D.; Mikuriya, M.; Handa, M. *Chem. Lett.* **2002**, *31*, 1044.
(4) (a) Cotton, F. A.; Walton, R. A. In *Multiple Bonds between Metal Atoms*, 2nd ed.; Clarendon Press: Oxford, U.K., 1993; p 18.(b) Miskowiski, V. M.; Hopkins, M. D.; Winkler, J. R.; Gray, H. B. In *Inorganic Electronic Structure and Spectroscopy*; Solomon, E. I., Lever, A. B. P., Eds.; John Wiley & Sons: New York, 1999; Vol. *2*, Chapter 6.(c) Norman, J. G.Jr.; Renzoni, G. E.; Case, D. A. *J. Am. Chem. Soc.* **1979**, *101*, 5256.
(5) (a) Telser, J.; Drago, R. S. *Inorg. Chem.* **1985**, *24*, 4765. (b) Telser, J.; Drago, R. S. *Inorg. Chem.* **1984**, *23*, 3114. (c) Cukiernik, F. D.; Giroud-Godquin, A. M.; Maldivi, P.; Marchon, J. C. *Inorg. Chim. Acta* **1994**, *215*, 203. (d) Handa, M.; Sayama, Y.; Mikuriya, M.; Nukada, R.; Hiromitsu, I.; Kasuga, K. *Bull. Chem. Soc. Jpn.* **1998**, *71*, 119. (e) Jimenez-Apraricio, R.; Urbanos, F. A.; Arrieta, J. M. *Inorg. Chem.* **2001**, *40*, 613.
(6) Cukiernik, F. D.; Luneau, D.; Marchon, J. C.; Maldivi, P. *Inorg. Chem.* **1998**, *37*, 3698.
(7) (a) Cotton, F. A.; Labella, L.; Shang, M. *Inorg. Chem.* **1992**, *31*, 2385. (b) Linday, A. J.; Wilkinson, G.; Motevalli, M.; Hursthouse, M. B. *J. Chem. Soc., Dalton Trans.* **1987**, *11*, 2723. (c) Yi, X.-Y.; Zheng, L.-M.; Xu, W.; Feng, S. *Inorg. Chem.* **2003**, *42*, 2827. (d) Liu, B.; Li, Y.-Z.; Zheng, L.-M. *Inorg. Chem.* **2005**, *44*, 6921. (e) Yi, X.-Y.; Liu, B.; Jiménez-Aparicio, R.; Urbanos, F. A.; Gao, S.; Xu, W.; Chen, J.-S.; Song, Y.; Zheng, L.-M. *Inorg. Chem.* **2005**, *44*, 4309. (f) Liu, B.; Yin, P.; Yi, X.-Y.; Gao, S.; Zheng, L.-M. *Inorg. Chem.* **2006**, *45*, 4205. (g) Liu, B.; Li, B.-L.; Li, Y.-Z.; Chen, Y.; Bao, S.-S.; Zheng, L.-M. *Inorg. Chem.* **2007**, *46*, 8524.
(8) McCann, M.; Murphy, E.; Cardin, C.; Convery, M. *Polyhedron* **1993**, *12*, 1725.
(9) (a) Zhilyaev, A. N.; Fomina, T. A.; Kuz'menko, I. V.; Rotov, A. V.; Baranovski, I. B. *Russ. J. Inorg. Chem.* **1989**, *34*, 532. (b) Kuz'menko, I. V.; Zhilyaev, A. N.; Fomina, T. A.; Porai-Koshits, M. A.; Baranovski, I. B. *Russ. J. Inorg. Chem.* **1989**, *34*, 1457. (c) Cotton, F. A.; Datta, T.; Labella, L.; Shang, M. *Inorg. Chim. Acta* **1993**, *203*, 55.

Published on Web 05/21/2009

magnetic materials, as it forms magnetically ordered systems with 3-D structures.[1a,1b] The Ni^{II} analogue was reported in a preliminary communication.[1b] Herein, we discuss the composition, structure, and magnetic behavior several M^{II} (M = Mn, Fe, Co, Ni, Cu, Mg) salts of $[Ru_2^{II/III}(CO_3)_4]^{3-}$.

Experimental Section

$M(NO_3)_2$ (M = Mn, Co, Ni, Cu), $Fe(SO_4)$, and $MgCl_2$ were used as purchased, and $K_3[Ru_2(CO_3)_4]$ was prepared via a literature route.[7a] Infrared spectra (± 1 cm^{-1}) were recorded on a Bruker Tensor 37 FT IR spectrometer. Elemental analyses were performed by Chemisar Laboratories and Atlantic Microlab, Inc.

Magnetic susceptibilities were measured in an 1000 Oe applied field between 2 and 300 K on a Quantum Design MPMS superconducting quantum interference device (SQUID) equipped with a reciprocating sample measurement system, low field option, and continuous low temperature control with enhanced thermometry features, as previously described.[10] Powder samples for magnetic measurements were loaded into gelatin capsules. The temperature dependence of the direct current (dc) magnetization was obtained by cooling in zero field and then the data were collected on warming in 5 Oe applied magnetic field. AC susceptibilities were measured at 10, 100, and 1000 Hz. In addition to correcting for the diamagnetic contribution from the sample holder, the core diamagnetic corrections of -264, -300, -297, -208, and -219×10^{-6} emu/mol were used for **1**−**5**, respectively.

Powder X-ray diffraction patterns were taken on a Bruker D8 Diffractometer (Cu Kα) using Mica (Standard Reference Material 675) for calibration. Additional powder diffraction measurements for Rietveld structure analysis were performed at Beamline X16C of the National Synchrotron Light Source at Brookhaven National Laboratory. The powdered sample was held in a 1.0 mm diameter thin-wall glass capillary. X-rays of wavelength 0.696677 Å were selected by a Si(111) channel cut monochromator. Diffracted X-rays were selected by a Ge(111) analyzer and detected by a NaI scintillation counter. The capillary was rotated during data collection for better averaging of the powder pattern data. The incident intensity was monitored by an ion chamber, and the measured signal was normalized. The TOPAS-Academic program was used to index, solve, and refine the structure by the simulated annealing method and subsequent Rietveld refinement.[11,12] The space group was hypothesized by checking the systematic absences of Pawley whole profile fitting. Rigid body constraints were imported to describe the paddlewheel structure of the Ru-dimeric cation, which follows the D_{4h} symmetry, but the interatomic distances were refined. Also, solvent molecules are necessary to explain the observed XRPD pattern, and K^+ (K13) and water [O^{2-}] (O14, O15) are present, and were used in the structure model; however, their occupancies and thermal parameters were refined freely; consequently, atom identifications are not meaningful in contrast to the framework building atoms.

Thermogravimetric analysis (TGA) was performed at a scan rate of 5 °C/min under a continuous 10 mL/min N_2 flow using a TGA 2050 TA Instruments located in a Vacuum Atmospheres DriLab under nitrogen to protect air- and moisture-sensitive samples.

$H_xK_{1-x}M^{II}[Ru_2(CO_3)_4](H_2O)_y(MeOH)_z$ ($0 \le x \le 1$) were synthesized using a 1.5:1 molar ratio of M^{II} salts and $K_3[Ru_2(CO_3)_4]\cdot 4H_2O$ (200 mg), each dissolved in 20 mL of H_2O. The solution of $K_3[Ru_2(CO_3)_4]$ was added to the stirred solution of M^{II} at the rate of 19.8 mL/h using a syringe pump. Syringe pump methods were employed to make the addition as uniform as possible, and slow addition with fast stirring minimizes formation of an initial black precipitate. After the addition was complete, a small amount of this feathery, black precipitate was removed via centrifugation.[13] Then MeOH was added to the highly colored supernatant to induce precipitation of the desired red-brown product, which was collected by centrifugation, washed with H_2O (and MeOH), and dried in a vacuum desiccator with Drierite and P_2O_5 overnight.

The product of nominal $H_xK_{1-x}M^{II}[Ru_2(CO_3)_4](H_2O)_y(MeOH)_z$ ($0 \le x \le 1$) composition with x, y, and z varying with preparation, and because of facile loss of solvent with time, was isolated. The formulas in bold below are the formulations obtained by combining the elemental analysis data with the thermogravimetric analysis (TGA) data and with the magnetic analysis (vide infra). The non-bolded formulas are based only upon the elemental analysis fitting. The elemental analysis data can be fit to several slight variations in the number of solvent molecules associated with the material, and thermogravimetric analysis (TGA) shows that significant solvent loss (5 ± 1 H_2O per Ru_2 for all samples) occurs readily at or just above room temperature. This is noted by a typical TGA scan (Supporting Information, Figure S1, M = Fe) that is characteristic of all compounds. Differences in the number of solvent molecules (x and y) also arise from solvent loss while sending samples in and out of glove boxes (for TGA), or during shipment for elemental analysis. All compounds nominally exhibit the same IR spectra.

[1]. M = Mn: $H_{0.3}K_{0.7}Mn[Ru_2(CO_3)_4](OH_2)_{5.5}$. IR (KBr, cm^{-1}): 1636, 1492(s), 1339, 1262(s), 1062(s), 817, 768, and 716 cm^{-1}. Anal. Calcd for $H_{0.3}K_{0.7}Mn[Ru_2(CO_3)_4](H_2O)_{2.7}(MeOH)_{0.2}$: $C_{4.2}H_{6.5}MnO_{14.9}K_{0.7}Ru_2$: C, 8.70; H, 1.13; N, 0.00; Obs: C, 8.69; H, 1.12; N, <0.2. Another sample was analyzed as: $H_{0.8}K_{0.2}Mn[Ru_2(CO_3)_4](OH_2)_{6.0}$: Anal. Calcd for $H_{0.8}K_{0.2}Mn[Ru_2(CO_3)_4](H_2O)_{2.6}$: $C_4H_{6.0}MnO_{14.6}K_{0.2}Ru_2$: C, 8.69; H, 1.09; N, 0.00; Obs: C, 8.70; H, 1.11; N, <0.2.

[2]. M = Fe: $H_{0.3}K_{0.7}Fe[Ru_2(CO_3)_4](H_2O)_6(MeOH)_{1.5}$. IR (KBr, cm^{-1}): 1630, 1489(s), 1267(s), 1063(s), 819, 766, and 717 cm^{-1}. Anal. Calcd for $H_{0.3}K_{0.7}Fe[Ru_2(CO_3)_4](H_2O)_{3.1}(MeOH)_{1.5}$: $C_{5.5}H_{12.5}FeO_{16.6}K_{0.7}Ru_2$: C, 10.49; H, 2.00; N, 0.00; Obs: C, 10.51; H, 2.01; N, <0.2.

[3]. M = Co: $KCo[Ru_2(CO_3)_4](H_2O)_8$. IR (KBr, cm^{-1}): 1633, 1493(s), 1339, 1263(s), 1063(s), 1006, 816, 764, and 714 cm^{-1}. Anal. Calcd for $KCo[Ru_2(CO_3)_4](H_2O)_{7.3}$ ($x = 0$): $C_4H_{14.6}CoO_{19.3}KRu_2$ Calc: C, 7.15; H, 2.19, N, 0.00; Obs: C, 7.15; H, 2.20, N, <0.2.

[4]. M = Cu: $KCu[Ru_2(CO_3)_4](H_2O)_{1.2}$. IR (KBr, cm^{-1}): 3435(br), 1633, 1485(s), 1461, 1313, 1268(s), 1066(s), 812, 784, and 717 cm^{-1}. Anal. Calcd for $KCu[Ru_2(CO_3)_4](H_2O)_{1.2}(MeOH)_{0.1}$: $C_{4.1}H_{2.8}CuO_{13.3}KRu_2$: C, 8.64; H, 0.50; N, 0.00; Obs: C, 8.63; H, 0.49; N, <0.2.

[5]. M = Mg: $H_{0.3}K_{0.7}Mg[Ru_2(CO_3)_4](H_2O)_3$. IR (KBr, cm^{-1}): 1645, 1489(s), 1338, 1263(s), 1063(s), 819, 764, and 714 cm^{-1}. Anal. Calcd for $H_{0.3}K_{0.7}Mg[Ru_2(CO_3)_4](H_2O)_{3.7}(MeOH)_{1.5}$: $C_{5.5}H_{13.7}MgO_{17.2}K_{0.7}Ru_2$: C, 10.85; H, 2.27; N, 0.00; Obs: C, 10.76; H, 2.15; N, <0.2.

Results and Discussion

Magnetically ordered materials of $M_3^{II}[Ru_2^{II/III}(CO_3)_4]_2$ composition were sought via the reaction of M^{II} and

(10) Brandon, E. J.; Rittenberg, D. K.; Arif, A. M.; Miller, J. S. *Inorg. Chem.* **1998**, *37*, 3376.

(11) *TOPAS V3: General profile and structure analysis software for powder diffraction data*, User's Manual; Bruker AXS: Karlsruhe, Germany, 2005; TOPAS-Academic is available at http://members.optusnet.com.au/~alancoelho.

(12) Coelho, A. A. *J. Appl. Crystallogr.* **2000**, *33*, 899.

(13) On the basis of the IR and PXRD data, this appears to be a disordered version of desired compound, and was not studied further.

$[Ru_2(CO_3)_4]^{3-}$ in as 3:2 ratio. It was hypothesized that the spins on the paramagnetic M^{II} ions would interact with the $S = 3/2$ Ru_2 core via the oxygens in a charge balancing 1.5:1 ratio. However, analysis of the structure revealed a material with the unexpected M/Ru_2 ratio of 1:1. This was observed for M = Ni, as preliminarily reported.[1b] Charge compensated $M^{2+}[Ru_2^{III/III}(CO_3)_4]^{2-}$ or $M^{3+}[Ru_2^{II/III}(CO_3)_4]^{3-}$ are unlikely because $[Ru_2^{III/III}(CO_3)_4]^{2-}$ is unstable in water,[7] and the expected structural distortions[14] (Jahn−Teller) of M(III) (M = Mn) species are not observed. The M^{II}:Ru_2^{3-} ratio leads to a formulation of $\{M[Ru_2(CO_3)_4]\}^-$, which is not charge compensated, and a proton and/or a potassium ion from the reaction media is assumed to be present to balance the charge as $H_x^+K_{1-x}^+M^{2+}[Ru_2^{II/III}(CO_3)_4]^{3-}(H_2O)_y(MeOH)_z$ {or $H_3O_x^+K_{1-x}^+M^{II}[Ru_2^{II/III}(CO_3)_4]^{3-}(H_2O)_y(MeOH)_z$}. This formulation is validated for M = Ni[1b] and for compounds **1** to **5** by elemental analysis data. The X-ray powder diffraction patterns for **1** to **3** and **5** show that they are isomorphous to that reported for M = Ni.[1b] Compound **4** (M = Cu) has a monoclinic unit cell, and its structure has not been elucidated (Table 1 and Supporting Information, Figure S2). Additionally, the presence of either M(III) or $[Ru_2^{III/III}(CO_3)_4]^{2-}$ can be ruled out based on the results of the magnetic data (vide infra).[15] However, because of disorder particularly in the lattice water, the refinement of the H positions is not possible. The presence of a H^+ for related systems, however, has been established, that is, $[Ru_2^{II/III}(O_2CMe)_4](O_2CMe{\cdot}HO_2CMe){\cdot}0.7H_2O$ with a H^+ bridge between two axial acetate oxygens[16] and $H[Ru_2(O_2CCH_3)_4(HPhPO_2)_2]$,[8] $H[Ru_2(O_2CCH_3)_4(PhPO_3H)_2]{\cdot}H_2O$,[8] and $K_2H[Ru_2(SO_4)_4(H_2O)_2]$.[9]

Structure. Attempts to grow single crystals were unsuccessful; however, high-resolution X-ray powder diffraction patterns (Supporting Information, Figure S3) were collected, and a Rietveld refinement of the data enabled the determination of the structure of the Mn species.[17]

The structure of **1** consists of a 3-D structural network composed of linked chains that differs from that observed for the layered $K_3[Ru_2(CO_3)_4]$ starting material.[7] Each $[Ru_2(CO_3)_4]^{3-}$ dimer contains four μ_3-carbonate ligands, with two of its oxygens bonding to the diruthenium moiety forming the typical paddlewheel (D_{4h}) geometry of the core, Figure 1a. The 2.265 Å Ru−Ru bond length is comparable to the 2.25 Å length reported for the starting material, and 2.258 Å observed for the Ni analogue.[1b] *trans* pairs of the third carbonate have oxygen atoms that bond to either a site axial to another Ru−Ru moiety via linkage **I**, as observed for $K_3[Ru_2(CO_3)_4]$,[7] or to an Mn^{II} via linkage **II** (Figure 1a) with an Mn−O−C angle of 128.5 ° and a Mn-OC separation of 2.107 Å. The pair of axial sites, with respect to the RuRu-bond, bonds to the carbonate oxygens (2.176 Å) from other anions, and have a RuRu−O−C angle of 139.2 °. The four $[Ru_2(CO_3)_4]^{3-}$ moieties that bond to $[Ru_2(CO_3)_4]^{3-}$ form a layered motif (Figure 1b). The layers are separated by the one-half of length of the *a*-axis, 9.4 Å for **1**. The remaining two *trans* carbonate oxygens bond to a $Mn(OH_2)_4$ unit (Figure 1a). Each six-coordinate manganese bonds *cis* to two ruthenium carbonate anions (92.7°) via linkage **II** (M = Mn), and four oxygens (average 2.18 Å) from H_2O molecules. The *cis* linkages form parallel 1-D chains in which adjacent chains are canted in different opposing directions (Figure 1c). These chains are linked together by one carbonate axially bonded to a Ru−Ru bond in another chain. The chain-linking Ru−O bond is shortened from 2.29 Å in $K_3[Ru_2(CO_3)_4]$ to 2.027 Å, indicating stronger interactions. **4** is not isomorphous, but its unit cell volume is comparable to the other members of this family (Table 3), and the Cu(II) site is less than six coordinate with fewer water molecules coordinated to it, and assumed to have a slightly altered structure.

Table 1. Orthorhombic Unit Cell Parameters for Isomorphous **1**−**3**, **5**, and for M = Ni, and Monoclinic **4** (M = Cu)

	Mn [**1**]	Ni[1b]	Fe [**2**]	Co [**3**]	Cu [**4**][b]	Mg [**5**]
a,[a] Å	18.77	18.19	18.46	18.35	10.71	18.42
b, Å	9.37	9.36	9.35	9.35	13.32	9.40
c, Å	10.09	10.05	10.04	10.06	11.90	10.02
V, Å^3	1774.6	1711.1	1732.9	1726.0	1675.0	1734.9

[a] Interlayer separation = *a*/2. [b] Monoclinic, non-isomorphous; β = 80.56°.

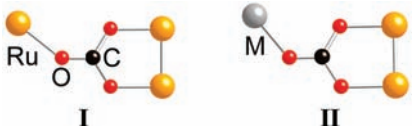

I II

Magnetic Properties. The magnetic susceptibility, χ, of $H_xK_{1-x}M^{II}[Ru_2(CO_3)_4](H_2O)_y(MeOH)_z$ (M = Mn, Fe, Co, Cu; $0 \le x \le 1$) was plotted as $\chi T(T)$, Figure 2 and Supporting Information, Figure S4. The 300 K χT values are 6.37, 6.29, 5.81, and 2.45 emuK/mol for **1**, **2**, **3**, and **4**, respectively. In all cases χT gradually decreased upon cooling, and reached a minimum at ∼50 K or below, and upon further cooling $\chi T(T)$ rapidly increased. The gradual decrease below 300 K is attributed to the large zero field splitting (D) associated with the anion.[4b] The $\chi T(T)$ data can be fit to an expression, eq 1, that accounts for D, as previously reported for other related Ru_2 compounds where N is Avogadro's number, k_B Boltzmann's constant, μ_B the Bohr Magneton, g the Landé g value, and TIP is the temperature independent paramagnetism.[18] The Weiss constant, θ, is also introduced to account for intermolecular magnetic interactions. The magnetic data was evaluated based on the bold-type formulas discussed earlier. Above 50 K the $\chi T(T)$ data is fit to eq 1 with D/k_B = 100 K, and g_{Ru2} = 2.02 and the parameters listed in Table 2. The D and g values were set to values previous reported

(14) Cotton, F. A.; Wilkinson, G.; Murillo, C. A.; Bochmann, M. *Advanced Inorganic Chemistry*, 6th ed.; John Wiley & Sons: New York, 1999; p 847.

(15) Attempts to fit the $\chi T(T)$ data to either $Ni^{3+}[Ru_2^{II/III}(CO_3)_4]_3{\cdot}3.35H_2O$ [with low spin Ni(III)], or $Ni^{2+}[Ru_2^{III/III}(CO_3)_4]_2{\cdot}3.35H_2O$ [with S = 1 or 2 Ru_2(III)] formulations required unreasonable g-values, and gave poor fits.

(16) Cotton, F. A.; Matusz, M.; Zhong, B. *Inorg. Chem.* **1988**, *27*, 4368.

(17) Chemical formula: $C_4H_8MnO_{16}Ru_2$, space group = *Pccn* (No. 56); a = 18.7729(2) Å, b = 9.3697(1) Å, c = 10.0946(1) Å, V = 1775.61(3) Å^3, Z = 4, ρ = 2.455(4) g/cm^3, T = 295 K, R_{ap} = 0.042, R_{wp} = 0.052, GoF = χ = 1.813.

(18) (a) Telser, J.; Drago, R. S. *Inorg. Chem.* **1985**, *24*, 4765. (b) Telser, J.; Drago, R. S. *Inorg. Chem.* **1984**, *23*, 3114.

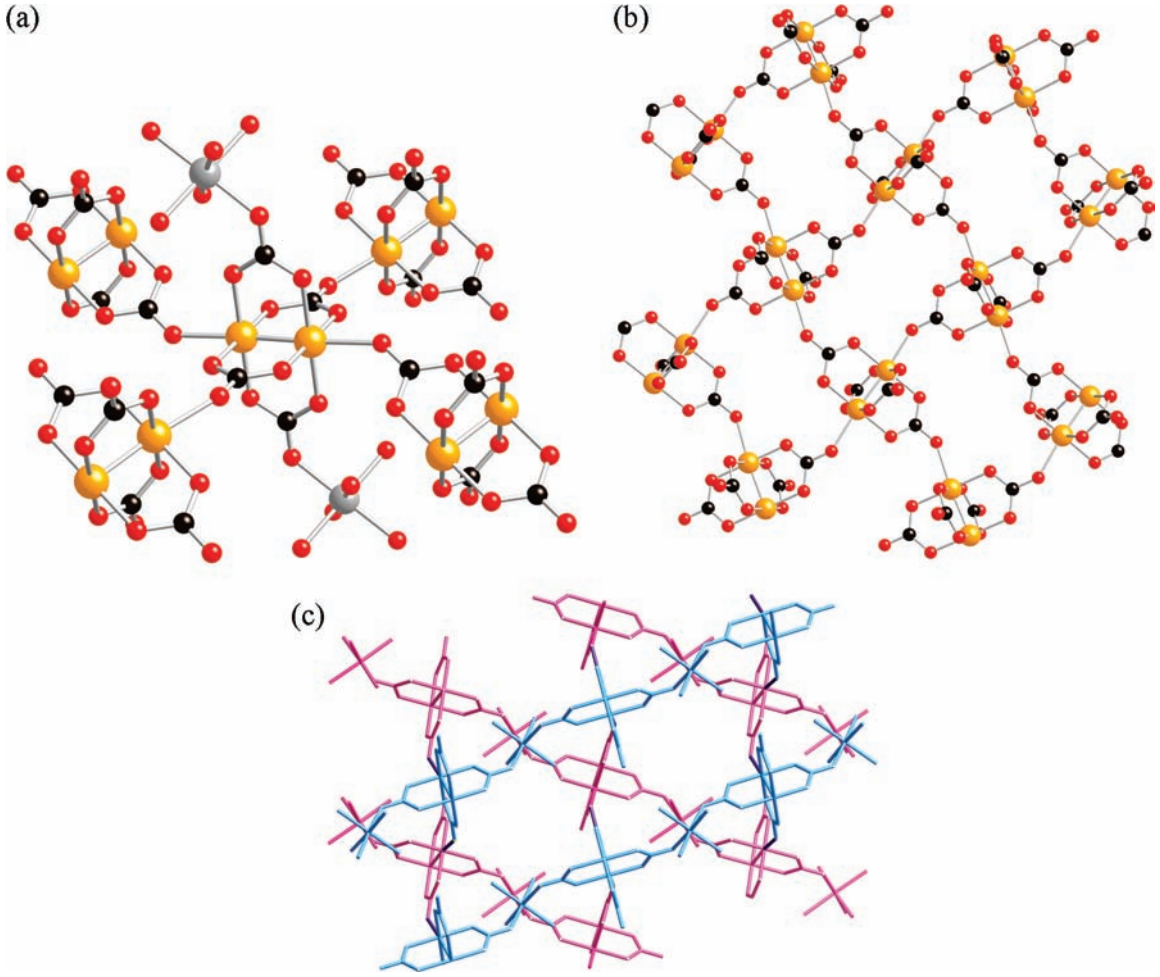

Figure 1. Structure of **1** consisting of $[Ru_2(CO_3)_4]^{3-}$ bonding to four additional $[Ru_2(CO_3)_4]^{3-}$ anions via type **I** linkages (a) that form a layered motif (b). These layers (b) are lined via $Mn(OH_2)_4$ type-**II** linkages (c).

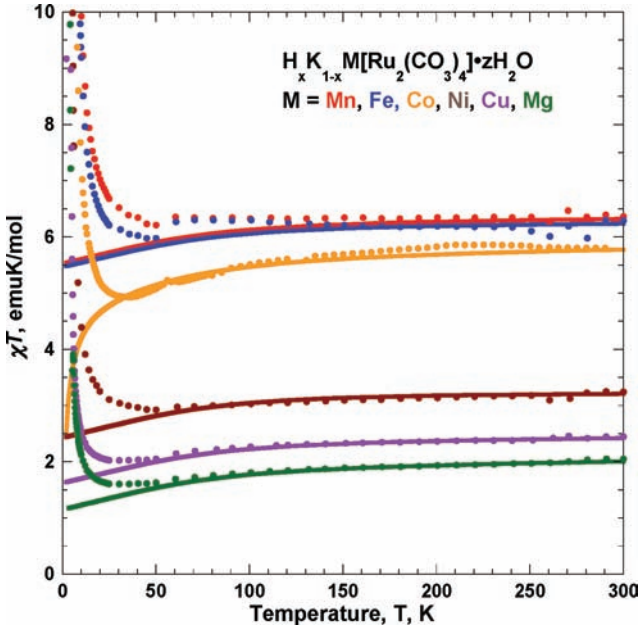

Figure 2. $\chi T(T)$ data with fit or high-temperature data with eq 1 as solid lines for $H_{0.3}K_{0.7}Mn(OH_2)_4[Ru_2(CO_3)_4]\cdot 1.5H_2O$ [**1**], $H_{0.3}K_{0.7}Fe(OH_2)_4(MeOH)_{1.5}[Ru_2(CO_3)_4]\cdot 2H_2O$ [**2**], $KCo(OH_2)_4[Ru_2(CO_3)_4]\cdot 4H_2O$ [**3**], $KCu(OH_2)_{1.2}[Ru_2(CO_3)_4]$ [**4**], $H_{0.3}K_{0.7}Mg(OH_2)_3[Ru_2(CO_3)_4]$ [**5**], and $HNi[Ru_2(CO_3)_4]\cdot 3.35H_2O$.[1b] See Supporting Information, Figure S4 for an expanded view of the data below 30 K.

Table 2. Magnetic Data Fitting Parameters for Equation 1

M^{II}	S	χT(300 K)$_{obs}$ (emuK/mol)	χT(300 K)$_{fit}$ (emuK/mol)	$g_{M(II)}$	θ (K)	TIP (μemu/mol)
[**1**] Mn	5/2	6.37	6.32	2.00	0	−200
[**2**] Fe	2	6.29	6.24	2.40	0	−100
[**3**] Co [a]	3/2	5.81	5.78	2.85	−2	−400
Ni [b]	1	3.24	3.22	2.20	0	−400
[**4**] Cu	1/2	2.45	2.42	2.25	0	−200
[**5**] Mg	0	2.05	2.01		0	−400

[a] Corrected for 3.9 ppm Co impurity. [b] Previously reported data for Ni compound fit with $g_{Ru2} = 2.08$ and TIP = 0;[1b] however, a better fit was obtained by refitting the data with the above values and $g_{Ru2} = 2.02$.

for related materials,[1,4,5c,5d,6,18] and were kept constant to enable useful comparison among the different cations.

$$\chi = \frac{Ng_{Ru_2}^2\mu_B^2}{k_B(T-\theta)}\left[\frac{1}{3}\cdot\frac{1+9e^{-2D/k_BT}}{4(1+e^{-2D/k_BT})} + \frac{2}{3}\cdot\frac{1+\frac{3k_BT}{4D}(1-e^{-2D/k_BT})}{1+e^{-2D/k_BT}}\right] + \frac{Ng_{M(II)}^2\mu_B^2(S)(S+1)}{3k_B(T-\theta)} + \text{TIP} \qquad (1)$$

Above 50 K the susceptibility is due to the single ion paramagnetism; however, the rapid rise at low temperature

Table 3. Summary of Important Magnetic Parameters for **1** to **5** and M = Ni

M^{II}	S	$T_c(\chi')$ (K)	$T_c(\chi'')$ (K)	T_b (K)	ϕ[19]	M_s (emu Oe/mol)	M_{rem} (emu Oe/mol)	H_{cr} (Oe)	χT(300 K) (emu K/mol)
[**1**] Mn	5/2	4.8[20]	5.4	6.0	0	31,400	940	32	6.37
[**2**] Fe	2	5.0	5.3	5.6	0	25,400	990	22	6.29
[**3**] Co	3/2	4.5	5.4	5.6	0	26,100	5,920	245	5.81
Ni	1	4.3	4.6	5.0	0	11,400	2,110	75	3.24
[**4**] Cu	1/2	4.1	4.3	5.4	0.012	12,300	385	28	2.45
[**5**] Mg	0	3.4	3.7	3.8	0	9,600	180	7.5	2.05

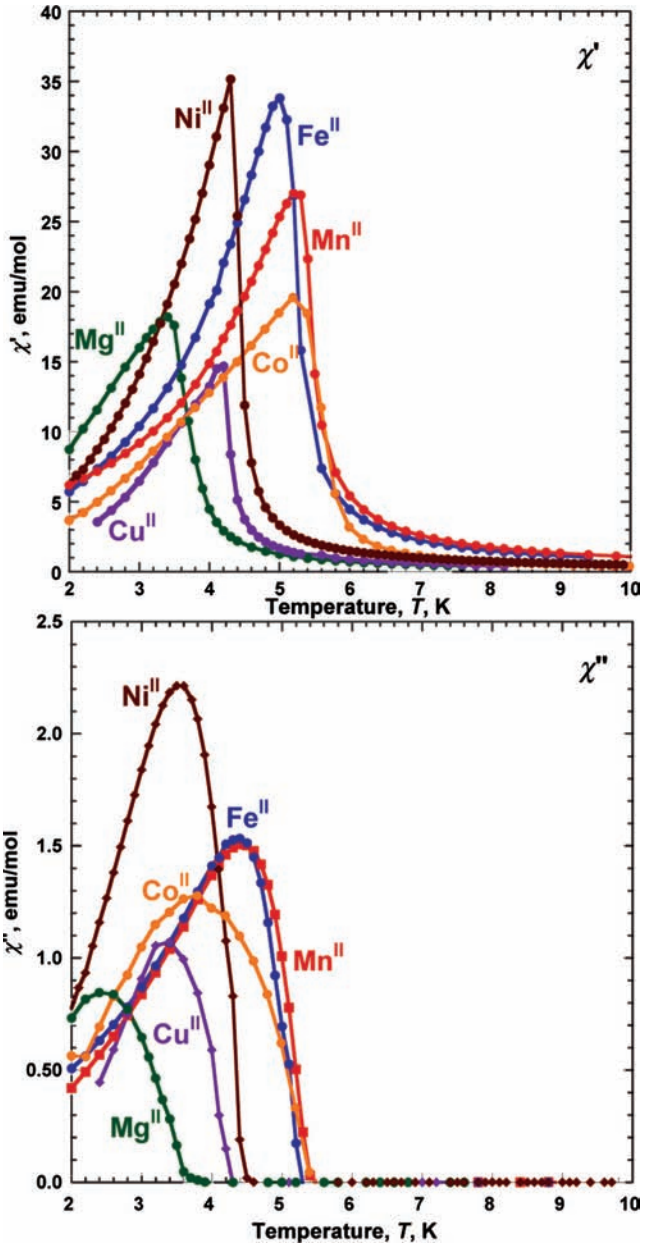

Figure 3. In-phase, $\chi'(T)$, and out-of phase, $\chi''(T)$, ac susceptibility data for $H_{0.3}K_{0.7}Mn(OH_2)_4[Ru_2(CO_3)_4]\cdot 1.5H_2O$ [**1**], $H_{0.3}K_{0.7}Fe(OH_2)_4(MeOH)_{1.5}[Ru_2(CO_3)_4]\cdot 2H_2O$ [**2**], $KCo(OH_2)_4[Ru_2(CO_3)_4]\cdot 4H_2O$ [**3**], $KCu(OH_2)_{1.2}[Ru_2(CO_3)_4]$ [**4**], $H_{0.3}K_{0.7}Mg(OH_2)_3[Ru_2(CO_3)_4]$ [**5**], and $HNi[Ru_2(CO_3)_4]\cdot 3.35H_2O$.[1b]

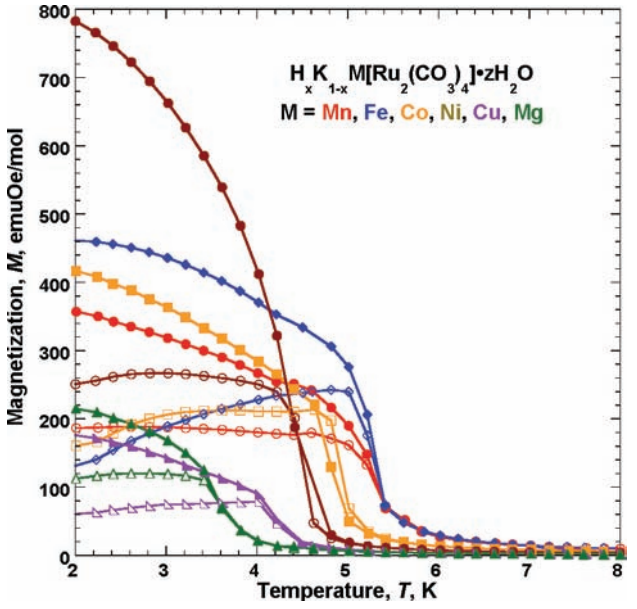

Figure 4. Zero field cooled (open symbols) and field cooled (solid symbols) data for $H_{0.3}K_{0.7}Mn(OH_2)_4[Ru_2(CO_3)_4]\cdot 1.5H_2O$ [**1**], $H_{0.3}K_{0.7}Fe(OH_2)_4(MeOH)_{1.5}[Ru_2(CO_3)_4]\cdot 2H_2O$ [**2**], $KCo(OH_2)_4[Ru_2(CO_3)_4]\cdot 4H_2O$ [**3**], $KCu(OH_2)_{1.2}[Ru_2(CO_3)_4]$ [**4**], $H_{0.3}K_{0.7}Mg(OH_2)_3[Ru_2(CO_3)_4]$ [**5**], and $HNi[Ru_2(CO_3)_4]\cdot 3.35H_2O$.[1b]

indicates magnetic ordering. Magnetic ordering was established from the temperature and frequency dependent in-phase, $\chi'(T)$, and out-of phase, $\chi''(T)$, alternating current (ac) susceptibility studies, Figure 3. Frequency independent absorptions in both the $\chi'(T)$ and the $\chi''(T)$ data were observed for $H_xK_{1-x}M^{II}(OH_2)_4[Ru_2(CO_3)_4]\cdot zH_2O$, except for non-isomorphous M = Cu (which exhibits slight dependence with $\phi = 0.012$ suggestive of a mild spin- or cluster-glass behavior[19]). Hence, they magnetically order, as is also reported for both $[Ru_2(O_2CMe)_4]_3[Cr(CN)_6]$[1d,1e] and $[Ru_2(O_2CBu^t)_4]_3[Cr(CN)_6]$,[1c] in addition to the Ni analogue.[1b] The magnetic ordering temperatures are determined by the peak in the 10 Hz $\chi'(T)$ data and are 4.8,[20] 5.0, 4.5, and 4.1 K for **1**, **2**, **3**, and **4**, respectively. Alternatively, the T_c can be taken as the rise in $\chi''(T)$, and this method gives comparable values of 5.4, 5.3, 5.4, and 4.3 K, for **1**, **2**, **3**, and **4**, respectively (Table 3).

The zero field cooled and field cooled (ZFC/FC) $M(T)$ data taken at 5 Oe have bifurcation temperatures, T_b, of 6.0, 5.6, 5.6, and 5.4, K for **1** to **4** (Figure 4) that are also consistent with magnetic ordering.

The magnetization at 5 T approaches saturation and is 31,400, 25,400, 26,100, and 12,300, emu Oe/mol for **1** to **4**, respectively (Figure 5). The spin-only expected values for ferromagnetic coupling between M^{II} and $[Ru_2(CO_3)_4]^{3-}$ are 44,700, 39,100, 33,500, and 22,350 emuOe/mol for

(19) Mydosh, J. A. In *Spin Glasses: An Experimental Introduction*; Taylor and Francis: London, **1993**, p 67. ϕ is a parameter indicative of the amount of spin disorder in a spin-glass: $\phi = \Delta T_{max}/[T_{max}(\Delta\log\,\omega)]$, where ΔT_{max} = difference between maximum peak of the temperatures at the high and low frequencies, T_{max} = peak maximum of the temperature at low frequency, $\Delta\log\,\omega$ = difference in the logarithms of the high and low frequencies (ω).

(20) Other samples of **1** have exhibited a T_c as high as 5.4 K, but collection of its complete magnetic data set was not possible.

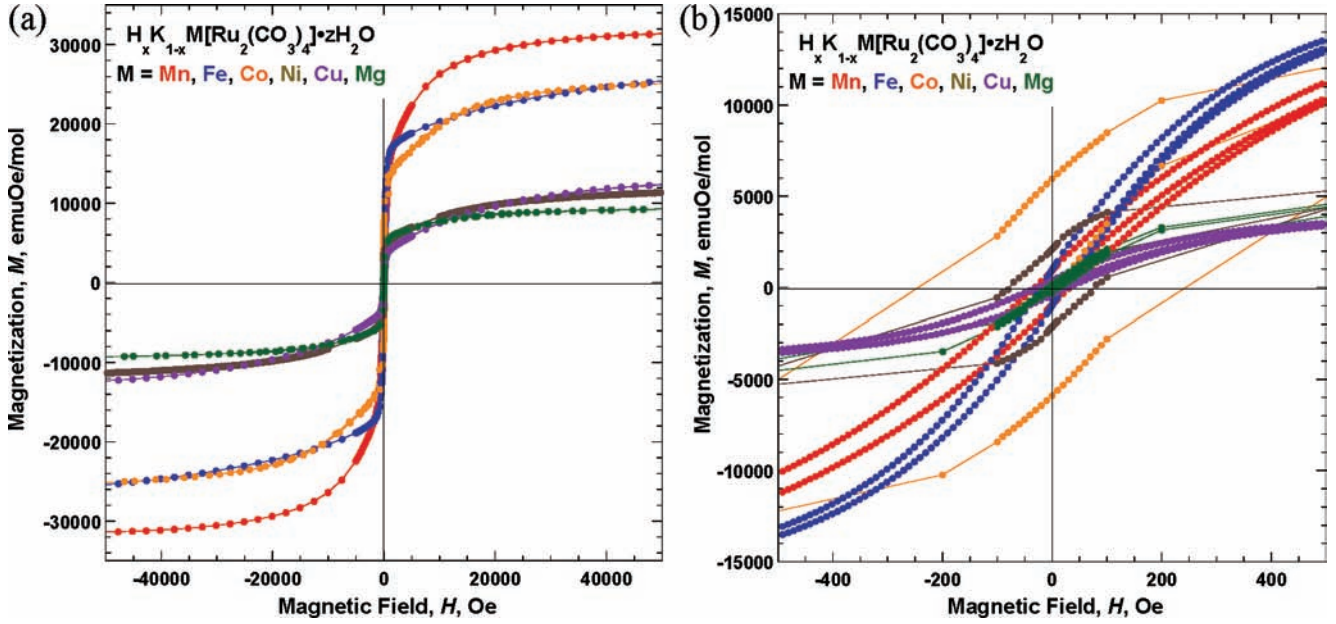

Figure 5. Hysteresis loop (±50,000 Oe) (a) and ±500 Oe (b) for $H_{0.3}K_{0.7}Mn(OH_2)_4[Ru_2(CO_3)_4]\cdot 1.5H_2O$ [**1**], $H_{0.3}K_{0.7}Fe(OH_2)_4(MeOH)_{1.5}[Ru_2(CO_3)_4]\cdot 2H_2O$ [**2**], $KCo(OH_2)_4[Ru_2(CO_3)_4]\cdot 4H_2O$ [**3**], $KCu(OH_2)_{1.2}[Ru_2(CO_3)_4]$ [**4**], $H_{0.3}K_{0.7}Mg(OH_2)_3[Ru_2(CO_3)_4]$ [**5**], and $HNi[Ru_2(CO_3)_4]\cdot 3.35H_2O$.[Tb]

1 to **4**, respectively.[21] For antiferromagnetic coupling, which leads to ferrimagnetic behavior, between M(II) and $[Ru_2(CO_3)_4]^{3-}$ for **1** to **4**, the respective expected values are 11,170, 5585, 0, and 11,170 emuOe/mol. Each of the observed values, however, is intermediate between values expected from ferro- and antiferromagnetic coupling and is indicative of a canted antiferromagnet (weak ferromagnet),which for this system is best termed a canted ferrimagnet. Hysteresis is observed in the 2 K $M(H)$ data for **1** to **4** with a coercive fields of 32, 22, 245, and 28 Oe, respectively (Figure 5). Remnant magnetizations, M_{rem}, of 940, 990, 5,920, and 385 emu Oe/mol for **1** to **4**, respectively, are also consistent with non-antiferromagnetic magnetic ordering. A summary of the important magnetic parameters is provided in Table 3.

The Mean Field model for 3-D ordered magnets shows that $T_c \propto JS(S+1)$,[22] but for a system with two different spins $T_c \propto [JS(S+1)S'(S'+1)]^{1/2}$.[1d,23] Assuming that the exchange coupling, J, is constant for an isostructural system, T_c should scale as 3.44:2.85:2.25:1.64:1 for Mn, Fe, Co, Ni, and Cu, respectively, that is, T_c(Mn) should be $\sim 3.44 \times T_c$(Ni) exceeding the observed value of 1.14. This is nominally in accord for $[Ru_2(O_2CMe)_4]_3[M(CN)_6]$ where $T_c(Cr^{III})/T_c(Fe^{III})$ is ~ 15; however, only a factor of 2.25 is expected from the Mean Field prediction.[1d] However, the T_c's for $M^{II}[Ru_2(CO_3)_4]$-based (M = Mn, Fe, Co, Ni, Cu) family remains essentially constant, that is,

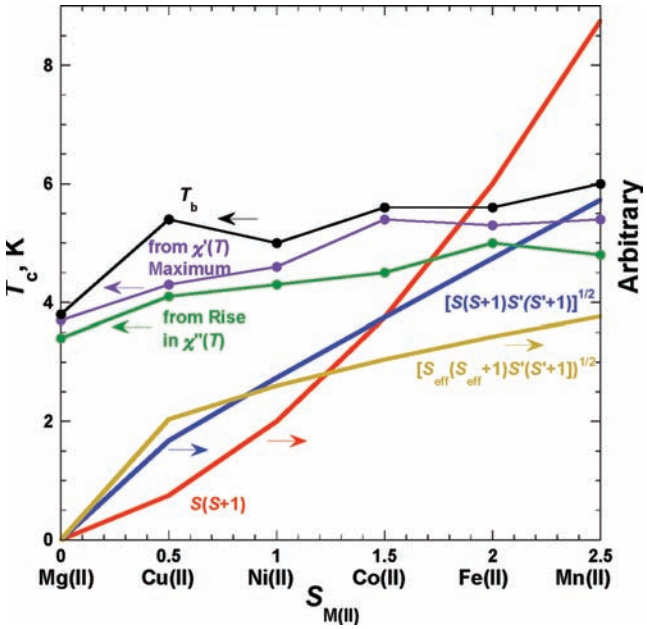

Figure 6. Nominal linear dependence of T_c and T_b as a function of S for **1**−**5** and for M = Ni. The lines between the data points are guides. The solid lines are trends predicted from the simple Mean Field model [i.e., $T_c \propto JS(S+1)$] (red),[22] a system with two different spins {i.e. $T_c \propto [JS(S+1)S'(S'+1)]^{1/2}$} (blue),[1d,23] or the latter system using an effective S, S_{eff}, of 1.15, because of the reduction of S arising from the large zero field splitting,{i.e. $T_c \propto [JS_{eff}(S_{eff}+1)S'(S'+1)]^{1/2}$} (brown).[1d]

5.5 ± 0.5 K, and does not scale as either $S(S+1)$ or $[S(S+1)S'(S'+1)]^{1/2}$ (Figure 6).[24] This suggests that the spins on these M^{II} cations do not contribute significantly to the magnetic coupling that leads to magnetic ordering but only to the paramagnetic susceptibility. To test this hypothesis that the bridging paramagnetic *cis*-$[M^{II}(OH_2)_4]^{2+}$ moiety does not contribute to the

(21) (a) These values are reduced by 6400 emu Oe/mol when the zero field splitting (D) is taken into account.(b) Shum, W. W.; Liao, Y.; Miller, J. S. *J. Phys. Chem. A* **2004**, *108*, 7460.

(22) Ashcroft, N. W.; Mermin, N. D. *Solid State Physics*; Saunders College Publishing: Philadelphia, PA, 1976; pp 715−718.

(23) (a) Verdaguer, M.; Bleuzen, A.; Marvaud, V.; Vaissermann, J.; Seuleiman, M.; Desplanches, C.; Scuiller, A.; Train, C.; Garde, R.; Gelly, G.; Lomenech, C.; Rosenman, I.; Veillet, P.; Cartier, C.; Villain, F. *Coord. Chem. Rev.* **1999**, *190*−*192*, 1023. (b) Tanaka, H.; Okawa, N.; Kawai, T. *Solid State Commun.* **1999**, *110*, 191. (c) Greedan, J. E.; Chien, C-L; Johnston, R. G. *J. Solid State Chem.* **1976**, *19*, 155. (d) Greedan, J. E. *J. Phys. Chem. Solids* **1971**, *32*, 819. (e) Kimishima, Y.; Ichiyanagi, Y.; Shimizu, K.; Mizuno, T. *J. Magn. Magn. Mater.* **2000**, *210*, 244.

(24) Because of the large zero field splitting for the anion, S for $[Ru^{II}/_2^{III}(O_2CO)_4]^{3-}$ is reduced to the effective value of 1.15.[1d] Using the $T_c \propto [JS_{eff}(S_{eff}+1)S'(S'+1)]^{1/2}$ relationship, likewise, does not scale.

magnetic ordering, the magnetic behavior of an isostructural material with a diamagnetic M^{II} ion was sought.

Diamagnetic Zn^{II} and Mg^{II} were identified, but the former did not form an isostructural material.[25] As discussed above Mg^{II}, **5**, is isostructural, and its orthorhombic unit cell parameters are listed in Table 1. The magnetic susceptibility data for **5** is shown in Figure 2 and is similar to that observed for **1**−**4** and for M = Ni. A good fit of the magnet data to eq 1 was obtained using the parameters listed in Table 2, resulting in an observed 300 K χT value of 2.05 emuK/mol. **5** exhibits a significant increase in χT(T) below ~50 K, also suggesting magnetic ordering, as observed for **1**−**4**. Magnetic ordering was determined by ac susceptibility studies, with **5** having absorptions in both $\chi'(T)$ and $\chi''(T)$ (Figure 3), and thus is also a canted ferrimagnet. The T_c for **5** is 3.4 K based on the peak in $\chi'(T)$, and is 3.7 K from the rise in $\chi''(T)$, Figure 6. In further agreement with magnetically ordered **1**−**4**, the ZFC/FC data for **5** (Figure 4) show a bifurcation temperature of 3.8 K. Hysteresis is observed in the $M(H)$ data for **5** (Figure 5), and the saturation magnetization is 9,600 emuOe/mol. This is lower than the ferro- and/or antiferromagnetic coupling value (the two values are identical as $S_{Mg(II)} = 0$) of 16,755 emuOe/mol and is additional evidence of canted ferrimagnetic behavior. Remnant magnetization and coercive field values of 180 emu Oe/mol and 7.5 Oe, respectively, were obtained for **5** that are in accord with a magnetically ordering material.

(25) Kennon, B. S.; Miller, J. S. unpublished results.

Conclusion

The aqueous reaction of $K_3[Ru_2(CO_3)_4]\cdot 4H_2O$ and M^{II} salts forms materials of H_xK_{1-x}-$M^{II}[Ru_2(CO_3)_4]$-$(H_2O)_y(MeOH)_z$ ($0 \leq x \leq 1$) composition, not a material with the expected 3:2 M/Ru_2 ratio. The structure consists of parallel layers separated by 9.25 ± 0.15 Å ($a/2$) (Figure 1b) whereby each $[Ru_2^{II/III}(CO_3)_4]^{3-}$ is bridged by four μ_3-CO_3^{2-} ligands (Type **I**), with interlayer bridging via *cis*-$[M^{II}(OH_2)_4]^{2+}$ moieties (Type **II**). These compounds magnetically order as canted ferrimagnets with very similar ordering temperatures of 4.4 ± 1.0 K, Figure 6. Surprisingly, this even occurs for diamagnetic, $S = 0$ M = Mg(II) and indicates that the bridging M(II) cation contributes to the 3-D network structure, but does not significantly contribute to the magnetic coupling pathways needed to stabilize magnetic ordering. Hence, this is a rare example of a magnet based upon a second row transition metal.

Acknowledgment. The authors gratefully acknowledge the helpful discussions with William W. Shum, and the support from the NSF (Grant 0553573). Use of the National Synchrotron Light Source, Brookhaven National Laboratory, was supported by the U.S. Department of Energy, Office of Basic Energy Sciences, under Contract No. DE-AC02-98CH10886.

Supporting Information Available: X-ray crystallographic data for $H_{0.3}K_{0.7}Mn[Ru_2(CO_3)_4](H_2O)_{5.5}$ (CCDC#720319) in CIF format. This material is available free of charge via the Internet at http://pubs.acs.org. It is also available free of charge via the Internet from the Cambridge Crystal Data Centre.